^{11}C-Acetate PET Imaging of Prostate Cancer

Nobuyuki Oyama, MD, PhD[1]; Hironobu Akino, MD, PhD[1]; Hiroshi Kanamaru, MD, PhD[1]; Yuji Suzuki, MD, PhD[1]; Satoshi Muramoto, MD[2]; Yoshiharu Yonekura, MD, PhD[3]; Norihiro Sadato, MD, PhD[4]; Kazutaka Yamamoto, MD, PhD[5]; and Kenichiro Okada, MD, PhD[1]

[1]Department of Urology, Fukui Medical University, Fukui, Japan; [2]Department of Radiology, Fukui Medical University, Fukui, Japan; [3]Biomedical Imaging Research Center, Fukui Medical University, Fukui, Japan; [4]National Institute for Physiological Sciences, Okazaki, Japan; and [5]Wakasa Energy Research Center, Fukui, Japan

^{11}C-Acetate can act as a probe of tissue metabolism through entry into catabolic or anabolic metabolic pathways as mediated by acetyl–coenzyme A. The uptake of ^{11}C-acetate in prostate cancer was investigated to determine whether this tracer has potential in tumor identification. **Methods:** Twenty-two patients with prostate cancer underwent PET after intravenous administration of 740 MBq ^{11}C-acetate. Eighteen of the 22 patients were also investigated with ^{18}F-FDG PET. Standardized uptake values (SUVs) for each tumor were investigated for tracer activity at 10–20 min after ^{11}C-acetate and 40–60 min after ^{18}F-FDG administration. **Results:** Adenocarcinoma of the prostate showed variable uptake of ^{11}C-acetate, with SUVs ranging from 3.27 to 9.87. In contrast, SUVs for ^{18}F-FDG ranged from 1.97 to 6.34. By visual inspection, ^{11}C-acetate accumulation in primary prostate tumors was positive in all patients, whereas ^{18}F-FDG accumulation was positive in only 15 of 18 patients. ^{11}C-Acetate PET in a patient with lymph node metastasis showed high intrapelvic accumulation corresponding to metastatic sites. Similarly, 2 patients with bone metastases were ^{11}C-acetate avid. **Conclusion:** ^{11}C-Acetate shows marked uptake in prostate cancer and is more sensitive in detection of prostate cancer than is ^{18}F-FDG PET. ^{11}C-Acetate represents a new tracer for detection of prostate cancer with PET, measuring radiopharmaceutical uptake pathways that are different from those measured by ^{18}F-FDG.

Key Words: prostate cancer; PET; ^{11}C-acetate

J Nucl Med 2002; 43:181–186

In tumor imaging using ^{18}F-FDG PET, ^{18}F-FDG is avidly taken up by tumor cells because cancer tissue consumes a large amount of glucose as an energy source (*1*). In general, tumors exhibit increased expression of glucose transporters (gluts), especially glut1 (*2*), and increased activity of hexokinase (HK), especially HK2 (*3*). Gluts transport glucose into cells, where it is phosphorylated by HK; ^{18}F-FDG enters tumor cells by the same transport route (*4*). ^{18}F-FDG PET has significantly changed the ability to diagnose ma-

lignant tumors. Because of the high glucose use of tumors, ^{18}F-FDG PET has been shown to be useful for the detection of many kinds of neoplasms, including those of the brain, head and neck, lung, and pancreas (*5–8*). ^{18}F-FDG PET is now widely being accepted as a highly effective means for imaging a wide variety of cancers (*9*).

The success of ^{18}F-FDG PET in many cancers has led to the evaluation of this radiopharmaceutical for use with prostate cancer. Prostate cancer is the most commonly diagnosed cancer in men and is the second leading cause of cancer death in men older than 40 y in the United States. Unfortunately, the primary disease within the prostate gland cannot be reliably imaged using ^{18}F-FDG (*10,11*). The poor performance of PET using ^{18}F-FDG is likely related to the low glucose metabolic rate that results from the relatively slow growth of most prostate cancers, as well as to other factors, including significant excretion of the tracer into the adjacent urinary bladder. In some cases, ^{18}F-FDG has been shown to have a relatively high sensitivity for detecting prostate cancer lesions, but only when there is high tumor viability, such as a high histologic grade, a high clinical stage, or a tumor in a patient with a high serum prostate-specific antigen (PSA) value (*11*). Although ^{18}F-FDG PET still has some value for staging prostate cancer when tumor viability is high, the limitations of ^{18}F-FDG require development of better imaging radiopharmaceuticals.

A second imaging technique for prostate cancer, scintigraphy using the radiolabeled monoclonal antibody ^{111}Incapromab pendetide (ProstaScint; Cytogen Corp., Princeton, NJ), has been introduced to aid in the diagnosis of prostate cancer. Although imaging with this radiopharmaceutical may be of value, the sensitivity and specificity still remain far from ideal, with most reports showing a range of 50%–70% for both measures (*12–14*).

Recently, PET using ^{11}C-acetate has been introduced in diagnosing cancer disease. Shreve et al. (*15,16*) reported that different histologic types of renal cell carcinomas showed high uptake of ^{11}C-acetate but differed markedly in the clearance of tissue tracer activity, which allows for the clear differentiation of the neoplasm from normal tissue on image frames beyond 10 min after tracer administration.

We have investigated the potential of ^{11}C-acetate to image prostate cancer. The purpose of this study was to

determine the feasibility of this tracer for detecting primary or metastatic prostate cancer lesions.

MATERIALS AND METHODS

Twenty-two patients (age range, 52–85 y; median age, 72.0 y) were enrolled in this study. Adenocarcinoma of the prostate was histologically diagnosed in these patients at Fukui Medical University between July 1997 and September 1999. Histologic diagnosis was through specimens obtained by a transrectal systematic sextant prostate biopsy. Clinical staging was according to the fifth edition of the *TNM Classification of Malignant Tumors* (*17*), and histologic grade was evaluated using the Gleason grading system (*18*). The serum PSA value was determined with a double monoclonal antibody radioimmunoassay (Tandem-R; Hybritech, Inc., San Diego, CA). PET studies were performed before the start of any type of treatment. In 8 patients, clinical stage T1/T2 was diagnosed; in 4, stage T3/T4; and in the remaining 10, stage $N(+)/M(+)$. Five of the 22 patients ultimately underwent a radical prostatectomy, including 1 patient who received endocrine therapy as neoadjuvant therapy. The other 17 did not require surgery and received only endocrine therapy with luteinizing hormone-releasing hormone agonist (3.6 mg goserelin) over a 28-d period. The protocol was approved by the Ethics Committee of Fukui Medical University. All patients were informed of the purpose of this study, the method of scanning, the time required, and the necessary pretreatment. Each consented to participate.

Patient Preparation

All patients underwent ^{11}C-acetate PET, and 18 patients also underwent ^{18}F-FDG PET within 1 wk. Each patient underwent ^{18}F-FDG PET after fasting for at least 4 h. During scanning, the bladder was irrigated continuously with 10 L physiologic saline through a 20 French 3-way balloon catheter, indwelt to prevent retention of ^{18}F-FDG in the bladder, enabling accurate evaluation of ^{18}F-FDG accumulation in the prostate.

PET Imaging Procedure

^{11}C-Acetate was produced from carbon dioxide by Grignard's reaction (*19*). ^{18}F-FDG was produced with the method of Hamacher et al. (*20*), using an automated ^{18}F-FDG synthesis system (NKK Corp., Tokyo, Japan) with a small cyclotron (OSCAR3; Oxford Instruments, Witney, U.K.). PET scanning was performed with an Advance system (General Electric Medical Systems, Milwaukee, WI). The physical characteristics of this scanner have been described in detail by DeGrado et al. (*21*). Two transmission scans covering the prostate and adjacent lower abdominal regions were obtained for 10 min each. A standard pin source of ^{68}Ge/^{68}Ga was used for attenuation corrections of the emission images.

A 740-MBq dose of ^{11}C-acetate was administered through the cubital vein over 10 s. Static images covering the prostate gland were obtained by scanning at 10–20 min after injection. A 350-MBq dose of ^{18}F-FDG was administered through the cubital vein over 10 s. Static scans covering the prostate were obtained at 40–60 min after injection.

Data Analysis

A circular region of interest (ROI) was placed on transaxial PET images at the location corresponding to the anatomic location of the prostate as shown on CT or MRI. The ROI location was determined in the area of highest accumulated radioactivity. As an index of ^{18}F-FDG uptake, the standardized uptake value (SUV) was calculated for each patient according to the following formula: SUV = radioactivity in ROI (Bq/cm^3)/injected dose (Bq)/body weight (g). We used the mean value of SUV within an ROI to represent ^{11}C-acetate and ^{18}F-FDG uptake in that particular region.

The PET images obtained were compared with images from other conventional modalities. The relationships between the accumulation of ^{11}C-acetate or ^{18}F-FDG and histologic grade, clinical stage, and serum PSA value were evaluated.

Statistical Evaluation

ANOVA was used to compare tracer uptake with the parameters of the prostate cancer. The correlation between SUV and serum PSA value was determined using Pearson's correlation coefficient.

RESULTS

Cancer Detection

Figure 1 shows images of a 71-y-old patient (patient 5) with an increased serum PSA value of 8.4 ng/mL. A trans-
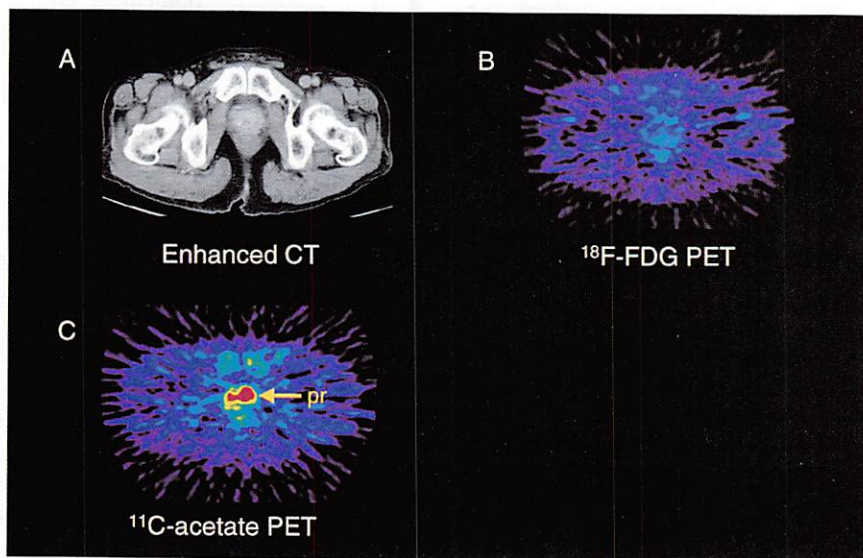

FIGURE 1. PET images of prostate obtained using ^{18}F-FDG and ^{11}C-acetate compared with CT image from 71-y-old man with well-differentiated (Gleason sum 2) adenocarcinoma of prostate. (A) CT shows only minimal enlargement of prostate. (B) ^{18}F-FDG PET shows low uptake in prostate, with SUV of 1.97. (C) ^{11}C-Acetate PET shows high uptake in primary prostate cancer lesion, with SUV of 6.41. pr = prostate

Enhanced CT

^{18}F-FDG PET

^{11}C-acetate PET

rectal needle biopsy of the prostate revealed well-differentiated adenocarcinoma with a Gleason sum of 2. CT showed mild prostate swelling without apparent capsular or seminal invasion. Bone scintigraphy did not show any high uptake within the bone. Both ^{11}C-acetate and ^{18}F-FDG PET were performed on this patient. ^{18}F-FDG PET showed only low uptake of the radiopharmaceutical in the prostate, with an SUV of 1.97, whereas ^{11}C-acetate PET showed higher uptake within the prostate, with an SUV of 6.41. A clinical stage of T2a N0 M0 was diagnosed, and a radical prostatectomy was performed. Surgically resected specimens revealed no capsular invasion, and no lymph node metastasis was seen.

Figure 2 shows the PET images of a 73-y-old patient (patient 6) with an increased serum PSA value of 92.8 ng/mL. A transrectal needle biopsy of the prostate revealed poorly differentiated adenocarcinoma with a Gleason sum of 7. Bone scintigraphy showed high uptake at the right pubic bone. MRI revealed a mass (2.5 cm in diameter) to the left of the urinary bladder. ^{11}C-Acetate PET and ^{18}F-FDG PET were performed on this patient. ^{18}F-FDG PET showed mild uptake of ^{18}F-FDG in the prostate, with an SUV of 2.87, whereas ^{11}C-acetate PET showed high uptake having an SUV of 5.45. ^{11}C-Acetate PET also showed high uptake in the right pubic bone, as well as left pelvic mass lesions that were also detected by ^{18}F-FDG PET. Both extraprostate lesions were considered to be bone and lymph node metastases. A clinical stage of T3c N2 M1 was diagnosed, and androgen ablation therapy was prescribed.

In all 22 patients, ^{11}C-acetate PET showed primary prostate cancer lesions and no ^{11}C-acetate accumulation in the urine (sensitivity, 100%). Of the 18 patients who were imaged with ^{18}F-FDG, primary lesions were seen in 15 of 18 (sensitivity, 83%). The remaining patient could not be evaluated because of high ^{18}F-FDG retention in the bladder. Of the 5 patients who had lymph node metastases, ^{11}C-acetate

PET showed all to have high intrapelvic accumulations corresponding to metastatic sites. These intrapelvic accumulations were seen in only 2 of the 5 patients when ^{18}F-FDG was used for imaging. Seven of the patients in the test group were found to have bone metastases, which were detected with ^{99m}Tc-hydroxymethylene diphosphonate bone scintigraphy (Table 1). Of these 7, 6 showed high ^{11}C-acetate accumulation at the site of the bone metastases, compared with 4 in whom high accumulation was seen when ^{18}F-FDG was used as the tracer compound (Table 2).

Evaluation of Tumor Viability

The relationship between the accumulation of ^{11}C-acetate or ^{18}F-FDG and clinical parameters was evaluated (Fig. 3). No correlations existed between the Gleason sum and ^{11}C-acetate or ^{18}F-FDG uptake. Patients with an advanced clinical stage of primary prostate cancer showed higher ^{18}F-FDG uptake than did patients with earlier stages ($P = 0.03$). No correlation was seen between clinical stage and ^{11}C-acetate uptake. A weak correlation was found between ^{18}F-FDG uptake and the serum PSA value ($r = 0.71$).

DISCUSSION

Conventional imaging modalities such as sonography, CT, and MRI are used for the anatomic evaluation of prostate cancer. However, visible anatomic changes are not always present in early stages, making use of these imaging modalities difficult in early detection of prostate cancer sites.

^{18}F-FDG PET for cancer diagnosis has been introduced as a metabolic imaging technique on the basis of the large amount of glucose that cancer tissue, in general, consumes as an energy source. However, for the diagnosis of prostate cancer, ^{18}F-FDG PET has no value in comparison with conventional diagnostic modalities such as PSA, CT, or MRI. The 60%–70% sensitivity previously shown for can-
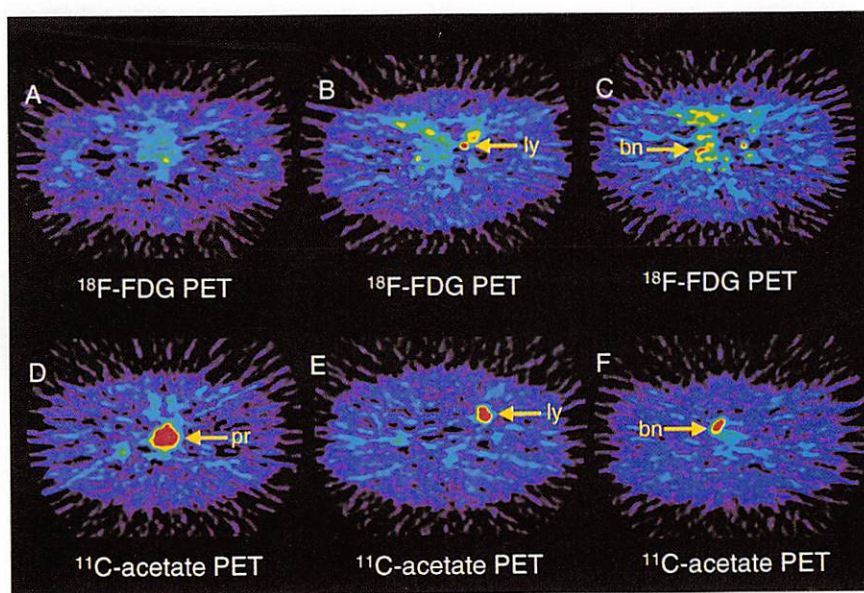

FIGURE 2. PET images of prostate, lymph node, and bone metastases obtained using ^{18}F-FDG and ^{11}C-acetate from 73-y-old man with poorly differentiated (Gleason sum 7) adenocarcinoma of prostate. (A) ^{18}F-FDG PET shows low uptake in prostate, with SUV of 2.87. (B and C) ^{18}F-FDG uptake was shown in left iliac lymph node metastatic lesion (B) and right pubic bone metastatic lesion (C). (D–F) ^{11}C-Acetate PET shows high uptake in prostate (D), with SUV of 5.45; in left iliac lymph node metastatic lesion (E); and in right pubic bone metastatic lesion (F). bn = bone; ly = lymph node; pr = prostate.

TABLE 1
Patient Details and Uptake of ^{11}C-Acetate and ^{18}F-FDG

Patient no.	Age (y)	PSA (ng/mL)	Gleason sum	Clinical stage	^{11}C-Acetate SUV	^{11}C-Acetate Uptake	^{18}F-FDG SUV	^{18}F-FDG Uptake
1	68	170.0	9	T4a N0 M1	6.09	Positive Bone-positive	5.34	Positive Bone-positive
2	67	16.0	9	T2b N0 M0	5.64	Positive	3.02	Positive
3	73	57.1	6	T3b N0 M0	4.24	Positive	4.46	Positive
4	69	69.5	6	T3c N0 M0	7.81	Positive	NA	
5	71	8.4	2	T2a N0 M0	6.41	Positive	1.97	Negative
6	73	92.8	7	T3c N2 M1	5.45	Positive Lymph node–positive Bone-positive	2.87	Negative Lymph node–positive Bone-positive
7	74	24.0	8	T4a N0 M1	5.69	Positive Bone-negative	4.47	Positive Bone-negative
8	75	6.8	2	T1a N0 M0	3.27	Positive	2.52	Negative
9	52	36.8	5	T2b N0 M0	7.22	Positive	3.09	Positive
10	72	42.1	7	T3a N0 M0	4.31	Positive	3.93	Positive
11	72	13.6	5	T1c N0 M0	3.83	Positive	2.57	Positive
12	73	91.2	3	T3c N0 M0	7.34	Positive	4.37	Positive
13	80	8.0	5	T2b N0 M0	5.02	Positive	3.19	Positive
14	62	207.0	Unknown	T3c N1 M1	5.39	Positive Lymph node–positive Bone-positive	3.06	Positive Lymph node–negative Bone-negative
15	70	203.0	7	T3c N1 M1	7.11	Positive Lymph node–positive Bone-positive	6.34	Positive Lymph node–positive Bone-positive
16	85	59.2	6	T3c N0 M1	5.75	Positive Bone-positive	3.57	Positive Bone-negative
17	67	29.5	6	T3c N1 M0	3.41	Positive Lymph node–positive	3.10	Positive Lymph node–negative
18	77	8.5	3	T2b N0 M0	5.65	Positive	NA	
19	60	296.0	7	T3c N0 M1	9.60	Positive Bone-positive	5.90	Positive Bone-positive
20	78	77.7	7	T4a N0 M0	9.87	Positive	NA	
21	67	1.9	3	T2a N0 M0	3.42	Positive	NA	
22	81	49.7	6	T4a N1 M0	8.55	Positive Lymph node–positive	3.24	Positive Lymph node–negative

NA = not available.
Positive stands for positive tracer uptake for primary prostate cancer site.

cer detection is not high enough to justify the clinical application of ^{18}F-FDG PET for the detection of prostate cancer, given the expense of ^{18}F-FDG PET over conventional methods (10,11).

[11]C-Acetate has been known as a positron-emitting tracer for measuring oxidative metabolism in the myocardium. As

TABLE 2
Detection of Prostate Cancer Lesions by PET

Cancer sites	^{11}C-Acetate No. of lesions detected	%	^{18}F-FDG No. of lesions detected	%
Primary lesions	22/22	100	15/18	83
Lymph node metastases	5/5	100	2/5	40
Bone metastases	6/7	86	4/7	57

soon as the myocardium takes in ^{11}C-acetate, it is converted to acetyl–coenzyme A in the mitochondria, followed by rapid clearance as carbon dioxide through the citric acid cycle. Recently, ^{11}C-acetate has been reported to show high uptake in tumor tissue (15,16). The mechanism of high ^{11}C accumulation in tumor cells, although yet unknown, is thought to be different from that of myocardium uptake. Yoshimoto et al. (22) studied uptake of ^{14}C-acetate in 4 different tumor cell lines and a fibroblast cell line to investigate the metabolic pathway of ^{11}C-acetate in tumor cells. [14]C accumulation in each of the 4 tumor lines was higher than that in the fibroblast cells, and this accumulation in tumor cells was shown to be caused by enhanced lipid synthesis. Given the highly active basal lipid metabolism associated with the cell membrane because of tumor growth, ^{11}C-acetate may be an important probe of this anabolic pathway of metabolism in cancer tissue.
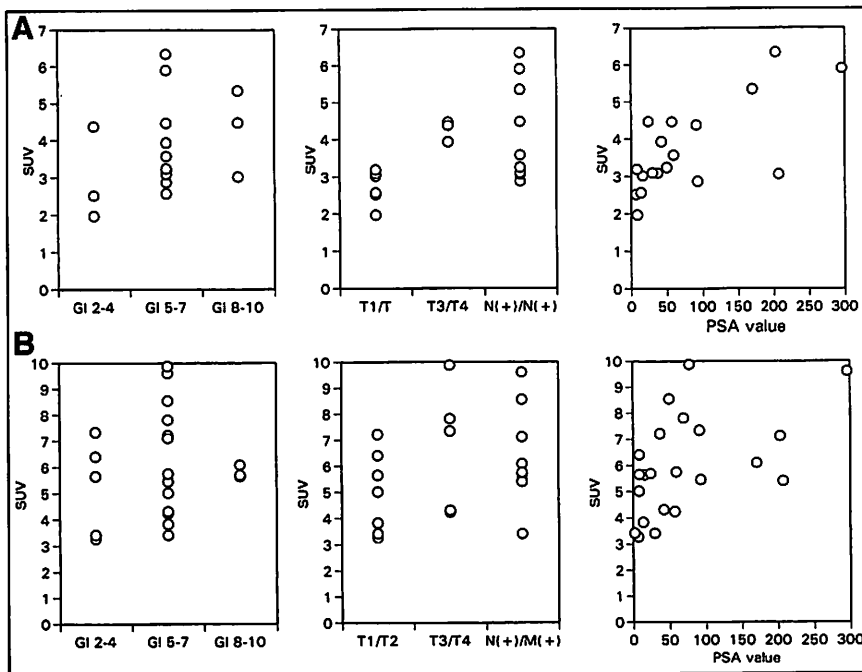
FIGURE 3. (A) No correlation was found between Gleason sum and ^{18}F-FDG uptake (P = 0.42). Patients with advanced-stage disease showed higher ^{18}F-FDG uptake than did those with earlier stages (P = 0.03). Weak correlation was found between ^{18}F-FDG and serum PSA value (r = 0.71). (B) No correlation was found among clinical parameters and ^{11}C-acetate uptake. Gl = Gleason sum.

The University of Michigan group (*23*), using ^{18}F-FDG and ^{11}C-acetate PET imaging, studied 18 prostate cancer patients who had rising PSA levels and bone scan or CT evidence of locally recurrent or regional metastatic disease. ^{11}C-Acetate PET showed high sensitivity for detecting both primary and nodal metastatic prostate cancer lesions. Tumor uptake of ^{11}C-acetate, as compared with ^{18}F-FDG, was found to be moderately high, and ^{11}C-acetate had higher sensitivity for tumor detection, without the confounding bladder activity of ^{18}F-FDG PET.

^{11}C-Acetate PET has been introduced as a new modality for imaging prostate cancer and its metastases (*23,24*). We found primary prostate cancer to be positive for ^{11}C-acetate accumulation in all patients imaged. In the meantime, the 83% sensitivity for detection of primary prostate cancer using ^{18}F-FDG was higher than previously reported (*10,11*). The high sensitivity found for ^{18}F-FDG PET may be the result of the relatively high proportion of patients with advanced-stage disease studied. ^{18}F-FDG PET has been reported to show higher sensitivity for detecting prostate cancer lesions of higher clinical stages (*11*). Indeed, in our 19 patients who underwent ^{18}F-FDG PET, the sensitivity was lower for localized disease than for advanced-stage disease (67% vs. 92%).

^{11}C-Acetate PET also showed high sensitivity for metastatic prostate cancer lesions. We investigated patients with confirmed metastases from prostate cancer; ^{11}C-acetate PET detected all known lymph node metastases and all bone metastases except 1. The high sensitivity of ^{11}C-acetate in prostate imaging will greatly help in detecting prostate cancer and extended metastases or sites of local recurrence, which are difficult to detect by conventional imaging modalities.

We also confirmed a previously reported (*11*) positive correlation between clinical stage and ^{18}F-FDG uptake in prostate cancer. This finding indicates that glucose use, shown by ^{18}F-FDG PET, is associated with progression of prostate cancer. On the contrary, this study found no relationship between the accumulation of ^{11}C-acetate and clinical parameters such as Gleason sum, clinical stage, and serum PSA value. This result cannot be explained by only the enhanced lipid metabolism that is associated with the cell membrane because of tumor growth. A further clinical study with a larger number of patients, as well as basic studies, is needed to clarify the mechanism of ^{11}C-acetate uptake in prostate cancer.

CONCLUSION

We evaluated ^{11}C-acetate as a potential PET tracer for imaging prostate cancer and found a marked uptake of ^{11}C-acetate into primary prostate cancer and metastatic sites, with higher sensitivity than that of ^{18}F-FDG PET. ^{11}C-Acetate is a promising tracer for imaging prostate cancer and its metastases. Further studies using ^{11}C-acetate PET with a larger number of patients are needed to determine its ultimate clinical utility.

ACKNOWLEDGMENTS

REFERENCES

1. Strauss LG, Conti PS. The applications of PET in clinical oncology. *J Nucl Med.* 1991;32:623–648.
2. Smith TAD. Facilitative glucose transporter expression in human cancer tissue. *Br J Biomed Sci.* 1999;56:285–292.
3. Adams V, Kempf W, Hassam S, Briner J. Determination of hexokinase isoenzyme I and II by RT-PCR: increased hexokinase II isoenzyme in human renal cell carcinoma. *J Biochem Mol Med.* 1995;54:53–58.
4. Smith T. FDG uptake, tumour characteristics and response to therapy: a review. *Nucl Med Commun.* 1998;19:97–105.
5. Pantonas NJ, Chiro GD, Kufta C, et al. Prediction of survival in glioma patients by means of positron emission tomography. *J Neurosurg.* 1985;62:816–822.
6. Rege S, Maass A, Chaiken L, et al. Use of positron emission tomography with fluorodeoxyglucose in patients with extracranial head and neck cancers. *Cancer.* 1994;73:3047–3058.
7. Nolop KB, Rhodes CG, Brudin LH, et al. Glucose utilization in vivo by human pulmonary neoplasms. *Cancer.* 1987;60:2682–2689.
8. Kato T, Fukatsu H, Ito K, et al. F-18-FDG-PET in pancreatic cancer: an unsolved problem. *Eur J Nucl Med.* 1995;22:32–39.
9. Rigo P, Paulus P, Caschten B, et al. Oncological applications of positron emission tomography with fluorine-18-fluorodeoxyglucose. *Eur J Nucl Med.* 1996;23:1641–1647.
10. Effert PJ, Bares R, Handt S, Wolff JM, Bull D, Jakes G. Metabolic imaging of untreated prostate cancer by positron emission tomography with 18-fluorine-labeled deoxyglucose. *J Urol.* 1996;155:994–998.
11. Oyama N, Akino H, Suzuki Y, et al. The increased accumulation of [^{18}F]fluoro-deoxyglucose in untreated prostate cancer. *Jpn J Clin Oncol.* 1999;29:623–629.
12. Seltzer MA, Barbaric Z, Belldegrun A, et al. Comparison of helical computerized tomography, positron emission tomography and monoclonal antibody scans for evaluation of lymph node metastases in patients with prostate specific antigen relapse after treatment for localized prostate cancer. *J Urol.* 1999;162:1322–1328.
13. Elgamal AA, Troychak MJ, Murphy GP, et al. ProstaScint scan may enhance identification of prostate cancer recurrence after prostatectomy, radiation, or hormonal therapy: analysis of 136 scans of 100 patients. *Prostate.* 1998;37:261–269.
14. Polascik TJ, Manyak MJ, Haseman MK, et al. Comparison on clinical staging algorithms and ^{111}indium-capromab pendetide immunoscintigraphy in the prediction of lymph node involvement in high risk prostate carcinoma patients. *Cancer.* 1999;85:1586–1592.
15. Shreve P, Chiao PC, Humes HD, Schwaiger M, Gross MD. Carbon-11-acetate PET imaging in renal disease. *J Nucl Med.* 1995;36:1595–1601.
16. Shreve PD, Gross MD. Imaging of the pancreas and related diseases with PET carbon-11-acetate. *J Nucl Med.* 1997;38:1305–1310.
17. Sobin LH. *TNM Classification of Malignant Tumors.* 5th ed. New York, NY: Wiley-Liss; 1997.
18. Gleason DF, for the Veterans Administration Cooperative Urological Research Group. Histologic grading and clinical staging of carcinoma of the prostate in urologic pathology. In: Tannenbaum M, ed. *The Prostate.* Philadelphia, PA: Lea and Febiger; 1997:171–197.
19. Kihlberg T, Valind S, Langstrom B. Synthesis of [1-^{11}C], [2-^{11}C], [1-^{11}C](2H3) and [2-^{11}C](2H3) acetate for in vivo studies of myocardium using PET. *Nucl Med Biol.* 1994;21:1067–1072.
20. Hamacher K, Coenen HH, Stocklin G. Efficient stereospecific synthesis of no-carried-added 2-[^{18}F]-fluoro-2-deoxy-D-glucose using aminopolyether supported nucleophilic substitution. *J Nucl Med.* 1986;27:235–238.
21. DeGrado TR, Turkington TG, Williams JJ, Stearns CW, Hoffman JM, Coleman RE. Performance characteristics of whole-body PET scanner. *J Nucl Med.* 1994;35:1398–1406.
22. Yoshimoto M, Waki A, Yonekura Y, et al. Characterization of acetate metabolism in tumor cells in relation to cell proliferation: acetate metabolism in tumor cells. *Nucl Med Biol.* 2001;28:117–122.
23. Shreve PD. Carbon-11 acetate PET imaging of prostate cancer [abstract]. *J Nucl Med.* 1999;40(suppl):60P.
24. Oyama N, Akino H, Kanamaru H, et al. C-11 acetate PET imaging of prostate cancer [abstract]. *J Urol.* 1999;161(suppl):392.